Einav, I. & Randolph, M. (2006). *Géotechnique* **56**, No. 7, 501–504

TECHNICAL NOTE

Effect of strain rate on mobilised strength and thickness of curved shear bands

I. EINAV* and M. RANDOLPH†

KEYWORDS: clays; piles; shear strength; stress analysis

INTRODUCTION

The shear strength of clays is strain-rate dependent, with the strength typically increasing by 5–20% for each order of magnitude increase in shear strain rate (Casagrande & Wilson, 1951; Graham *et al.*, 1983). This has a particular consequence for collapse problems in geotechnical engineering, where high velocity gradients exist in particular shear zones. These are generally idealised as localised surfaces across which step changes in velocity parallel to the surface occur, such as in the classical collapse mechanism for a strip footing (Prandtl, 1921). While this idealisation may be appropriate for soils that exhibit strain-softening, because strain localisation will lead to the formation of a sharp shear band a few soil particles wide (Roscoe, 1970; Vardoulakis & Graf, 1985), for soil that strain-hardens, or where the strength increases with strain rate, a diffuse shear band (or zone) will form. The rate of plastic work reduces as the change in velocity is spread over a greater shear band width.

For problems where the shear zone is curved, such as around a pile shaft or the cylindrical surface circumscribing a vane, it is possible to derive an optimum width of a notional shear band, and to quantify explicitly the maximum shear strain rate in terms of the change in tangential velocity and the internal (or minimum) radius of curvature of the shear band. This has application in assessing the effects of shearing rate for problems such as axial or torsional loading of piles, or in a conventional vane shear test (see Fig. 1).

MODELS FOR STRAIN-RATE DEPENDENCE OF STRENGTH

The effect of shear strain rate $\dot{\gamma}$ on the undrained shear strength s_u of clay may be expressed simply as

$$s_u = s_{u,ref}\left[1 + \lambda \log\left(\frac{\dot{\gamma}}{\dot{\gamma}_{ref}}\right)\right] \tag{1}$$

where λ is the rate of increase per decade, and $s_{u,ref}$ is a reference strength measured at a strain rate of $\dot{\gamma}_{ref}$ (Graham *et al.*, 1983).

There are sound arguments, both from physical principles (Mitchell, 1993) and to avoid problems as the strain rate approaches zero, for preferring an alternative version of the above relationship, based on an inverse hyperbolic sine function, expressed as

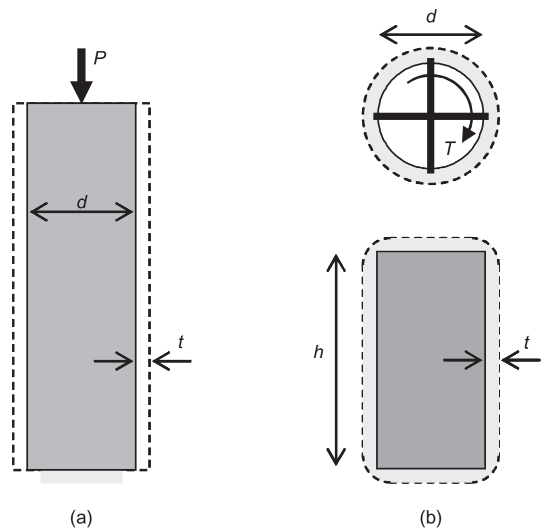

Fig. 1. Schematic of cylindrical shear bands: (a) pile under axial loading; (b) vane undergoing torsion

$$s_u = s_{u0}\left[1 + \lambda' \text{arc sinh}\left(\frac{\dot{\gamma}}{\dot{\gamma}_0}\right)\right] \tag{2}$$

Adopting $\lambda' = \lambda/\ln(10)$, this function reverts closely to equation (1) for strain rates in excess of the threshold rate, $\dot{\gamma}_0$, but leads to rapidly decaying strain rate effects for strain rates below $\dot{\gamma}_0$ so that, for strain rates below $0{\cdot}1\dot{\gamma}_0$, a minimum strength is reached that is about 4% lower than the value at $\dot{\gamma}_0$. The concept of a threshold strain rate below which the rate effect disappears has been noted by Sheahan *et al.* (1996); the subscript '0' has been used, rather than 'ref', to emphasise that s_{u0} is a true minimum shear strength at very low shear strain rates.

An alternative expression for the strength variation with strain rate is

$$s_u = s_{u,ref}\left(\frac{\dot{\gamma}}{\dot{\gamma}_{ref}}\right)^{\beta} \tag{3}$$

and this appears to capture well the tendency for the strain rate dependence to become more marked at higher rates of shearing. Biscontin & Pestana (2001) found that, for vane tests conducted at different rotation rates, the rate dependence in the vicinity of the conventional rotation rate of 0·1 deg/s was captured adequately using a logarithmic relationship with $\lambda \approx 0{\cdot}1$; at higher rates, however, the rate parameter increased to around 0·2, and better overall fits to the data were provided by the power law expression with values of β in the range 0·05–0·1. As for equation (1), a minimum shear strength would need to be specified at very low strain rates for practical application to typical soils.

Manuscript received 9 May 2005; revised manuscript accepted 24 May 2006.
Discussion on this paper closes on 1 March 2007, for further details see p. ii.
* School of Civil Engineering, University of Sydney, Australia (formerly at The University of Western Australia).
† Centre for Offshore Foundation Systems, The University of Western Australia, Crawley, Australia.

SIMPLE APPROACH FOR CURVED SHEAR BANDS

A simple non-rigorous energy approach, where equilibrium is not maintained within the shear band, allows estimation of the thickness of a curved shear band within a rate-dependent material by minimising the overall rate of work. For a shear band of inner radius of curvature r_0 and nominal width t, across which a velocity change Δv occurs, the average shear strain rate within the shear band is

$$\langle\dot{\gamma}\rangle = \frac{\Delta v}{t} \tag{4}$$

If this shear strain rate is assumed uniform across the shear band, the rate of plastic work may be estimated, and hence the shear band thickness that minimises the work may be calculated. Randolph (2004) showed that for a standard vane test, where $r_0 = 32{\cdot}5$ mm, with rotation rate of 0·1 deg/s and thus a velocity change of 0·06 mm/s, and adopting a reference shear strain of 1%/h (a typical laboratory testing rate), the thickness ratio is $t/r_0 \approx 0{\cdot}064$ for $\lambda = 0{\cdot}1$. Crucially, the existence of a non-zero optimal thickness for the shear band means that the shear strain rate is defined; in this case the average strain rate is $0{\cdot}029\ \mathrm{s}^{-1}$, or some 10^4 times greater than the reference rate of 1%/h ($2{\cdot}8 \times 10^{-6}\ \mathrm{s}^{-1}$).

The above result is dependent on the assumption that $\dot{\gamma} = \dot{\gamma}(r) = \langle\dot{\gamma}\rangle$, ignoring internal equilibrium. A more rigorous energy approach should leave the form of $\dot{\gamma} = \dot{\gamma}(r)$ unknown initially, but evaluated using a variational minimisation procedure. This technique is demonstrated in Appendix 1 for the power law rate dependence, and is addressed below by considering equilibrium directly.

RIGOROUS APPROACH MAINTAINING EQUILIBRIUM

Depending on the application, for example axial or torsional loading, the limiting shear stress (or rate-dependent shear strength) must vary in such a way as to maintain axial or torsional equilibrium, expressed as

$$\tau = \left(\frac{r_0}{r}\right)^n \tau_0 \tag{5}$$

where τ is the shear stress at radius r, with τ_0 being the value at r_0, while $n = 1$ for axial loading of a cylindrical pile, and $n = 2$ for torsional loading of a pile or vane. The shear strain rate within the shear band is given by

$$\dot{\gamma} = -r^{n-1}\frac{\mathrm{d}}{\mathrm{d}r}\left(vr^{1-n}\right) \tag{6}$$

where v is the axial or circumferential velocity.

Equilibrium may be maintained by allowing the shear strain rate to vary in such a way that the shear strength matches that required by equation (5). Rather than an explicitly defined shear band width, the shear strain rate will gradually reduce to zero, at a point where the shear strength has reduced to its minimum value. Essentially, both $\dot{\gamma}$ and v must merge to zero together.

In order to implement this approach, it is necessary to adopt a rate-dependence relationship that gives a finite shear strength at zero strain rate, for example the arc sinh or power law relationships in equations (2) and (3). The power law function will be looked at first, because it leads simply to an explicit function for the radial variation of velocity.

Power law rate dependence

Combining equations (3) and (5) leads to a condition on the shear strain rate, or velocity gradient, of

$$\dot{\gamma} = -r^{n-1}\frac{\mathrm{d}}{\mathrm{d}r}\left(vr^{1-n}\right) = \dot{\gamma}_{r_0}\left(\frac{r_0}{r}\right)^{n/\beta} \tag{7}$$

where $\dot{\gamma}_{r_0}$ is the shear strain rate at the inner edge of the shear band (where $r = r_0$). This may be integrated, enforcing a boundary condition of zero velocity at large radius, and a velocity of v_{r_0} at the inner edge, to give distributions of velocity and shear strain rate of

$$v = v_{r_0}\left(\frac{r_0}{r}\right)^{\frac{n-\beta}{\beta}} \tag{8a}$$

and

$$\dot{\gamma} = \left(\frac{n}{\beta} + n - 2\right)\frac{v_{r_0}}{r_0}\left(\frac{r_0}{r}\right)^{\frac{n}{\beta}} \tag{8b}$$

Alternatively, the above results may be recovered by minimising the energy and allowing for strain rate variations throughout the shear band, as detailed in Appendix 1. As it stands, the above indicates the existence of a diffuse shear zone, extending from $r = r_0$ to $r \to \infty$, rather than a shear band of finite thickness, because the form of the stress–strain law allows the strength to fall (artificially) to zero at very low strain rates. A shear band of finite width could be recovered by stipulating a minimum shear strength at low strain rates.

The shear strength mobilised at r_0 is then expressed as

$$s_\mathrm{u}(r_0) = s_\mathrm{u,ref}\left[\left(\frac{n}{\beta} + n - 2\right)\frac{v_{r_0}}{r_0\dot{\gamma}_\mathrm{ref}}\right]^{\beta} \tag{9}$$

Arc sinh rate dependence

Combining equations (2) and (5) leads to a relationship for the shear stress, or strength, with radius of

$$\frac{\tau}{\tau_0} = \left(\frac{r_0}{r}\right)^n = \left[1 + \lambda' \operatorname{arc\,sinh}\left(\frac{\dot{\gamma}}{\dot{\gamma}_0}\right)\right]\mathrm{A} \tag{10}$$

where

$$A = 1 + \lambda' \operatorname{arc\,sinh}\left(\frac{\dot{\gamma}_{r_0}}{\dot{\gamma}_0}\right)$$

This may be rearranged to give the shear strain, and hence velocity gradient, as

$$\dot{\gamma} = -r^{n-1}\frac{\mathrm{d}}{\mathrm{d}r}\left(vr^{1-n}\right) = \dot{\gamma}_0 \sinh\left[\frac{A(r_0/r)^n - 1}{\lambda'}\right] \tag{11}$$

This expression may be integrated numerically, from a known value of v at r_0, except that it is first necessary to assume a value for the shear strain rate at the inner boundary in order to evaluate A. The assumed value is then adjusted iteratively until the velocity reduces to zero at some radius where the strain rate is also zero. In contrast to the power law relationship in equation (8), the shear band has a finite thickness because the stress–strain relationship has a non-zero strength at zero strain rate. Thus, from equation (11), the outer radius of the shear band may be expressed as

$$r_\mathrm{outer} = r_0 A^{1/n} \tag{12}$$

EXAMPLE RESULTS

The analyses described above are compared here, taking a standard vane test as an example. Assumed parameters are for a vane of 65 mm diameter ($r_0 = 32{\cdot}5$ mm), rotating at 0·1 deg/s to give a peripheral velocity of $v_0 = 0{\cdot}057$ mm/s.

A reference shear strain rate of $\dot{\gamma}_0 = \dot{\gamma}_{ref} = 1\%/h$ ($2{\cdot}78 \times 10^{-6}\ s^{-1}$) is adopted.

Figure 2 compares velocity profiles for (a) the simple non-rigorous model with a linear variation of velocity (and thus constant shear strain rate) within a defined shear band width, and (b) the more consistent solutions taking either the arc sinh or power law rate dependence. The profiles are compared for axial ($n = 1$) and torsional ($n = 2$) deformation modes. As might be anticipated, the torsional deformation gives a more restricted shear band width, because the velocity gradient must decrease more rapidly with radius in order to maintain equilibrium. It is interesting that the simple approach gives a shear band width that, for practical purposes, is quite similar to the zone where most of the shearing occurs for the more rigorous approaches. The arc sinh model, taking $\lambda = 0{\cdot}15$ (so $\lambda' = 0{\cdot}065$), gives a slightly more rapid decay of velocity than the power law with $\beta = 0{\cdot}05$, but of course this would change if different relative magnitudes of λ and β were chosen.

Corresponding profiles of shear strain rate are shown in Fig. 3. For this case, in order to compare the axial and torsional modes, identical ratios of velocity v to inner radius r_0 have been adopted for both modes. (Note that a 2 m diameter pile displaced axially at 1·7 mm/s would have identical v/r_0 to a standard vane test.) Consistently with Fig. 2, the shear strain rates for torsional deformation are initially much higher than for axial deformation, by a factor of about 2. The arc sinh and power law models give quite similar profiles of shear strain rate for a given mode of deformation, and the simple model leads to a sensible average shear strain rate across the shear band width. The values corresponding to the torsional mode are consistent with the more detailed analysis of Pérez-Foguet *et al.* (1999), where the full geometry of the vane was modelled using an arbitrary Lagrangian-Eulerian (ALE) finite element formulation.

The net effects of different rates of shearing are compared for the standard vane test in Fig. 4, noting that only the contribution from the cylindrical surface is considered here, although that represents the major component of the torsional resistance (Chandler, 1988). Surprisingly, the simple non-rigorous approach performs quite well relative to the more rigorous arc sinh model, slightly underpredicting the enhancement of the torsional resistance, with progressively less accurate results for higher values of the rate parameter λ. The arc sinh and power law models also show reasonable consistency (for the chosen pairings of λ and β values), although the latter model gives much greater non-linearity on the semi-logarithmic plot at high values of β. This was noted also by Biscontin & Pestana (2001) in their fitting of vane test results.

It should be noted that, because of the varying width of the shear band, the net effect of a given rate dependence of the soil on the vane torque is less than if the same rate law is applied directly to the torque itself. This is illustrated in Fig. 5 for two

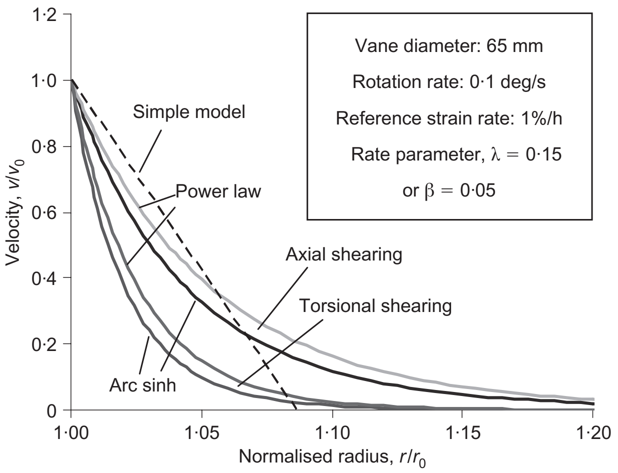

Fig. 2. Velocity profiles within shear band for all three models

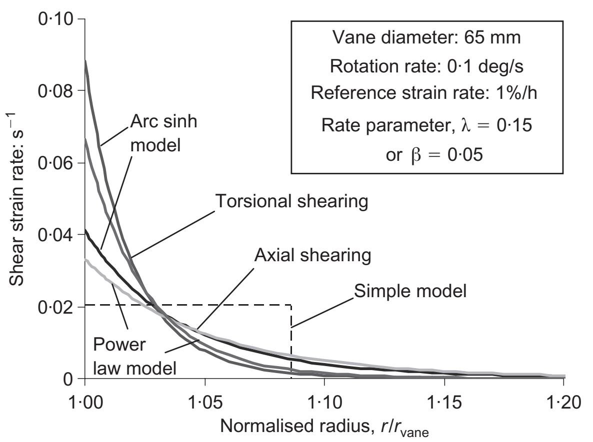

Fig. 3. Profiles of shear strain rate within shear band for all three models

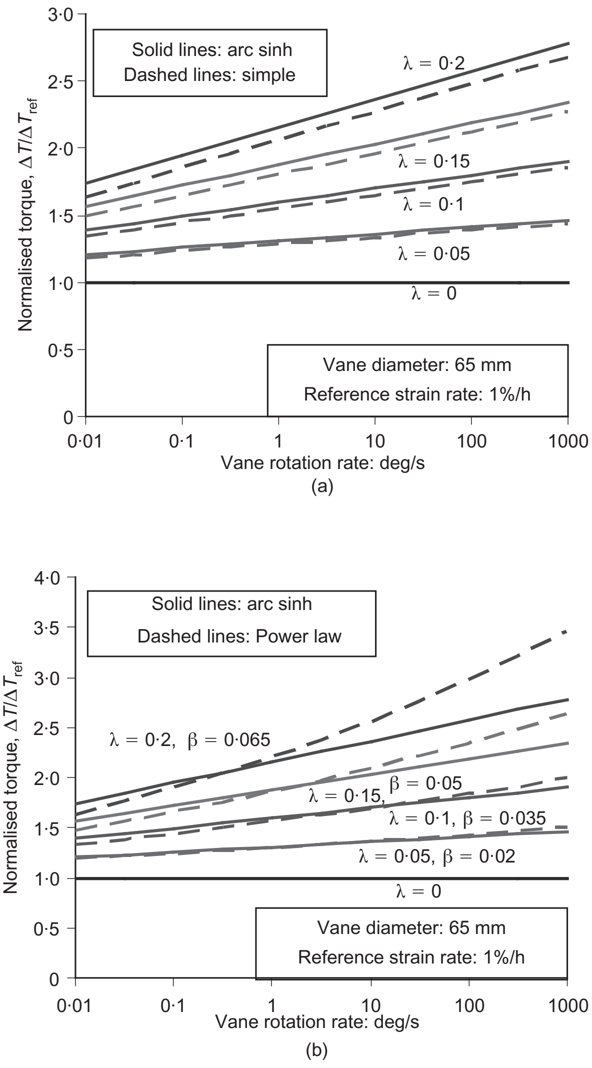

Fig. 4. Effect of vane rotation rate on torque: (a) comparison of arc sinh and simple model; (b) comparison of arc sinh and power law models

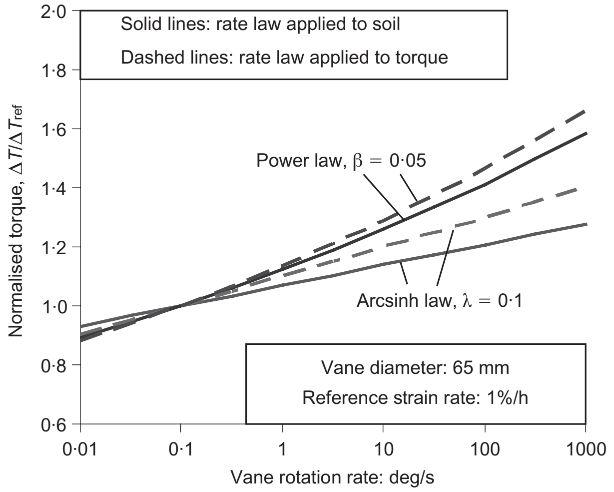

Fig. 5 Comparison of rate laws applied to soil or directly to vane torque

cases, where the dashed lines correspond to direct relationships of the form

$$\frac{\Delta T}{\Delta T_{\text{ref}}} = 1 + \lambda' \text{arc sinh}\left(\frac{\omega}{\omega_{\text{ref}}}\right) \tag{13}$$

or

$$\frac{\Delta T}{\Delta T_{\text{ref}}} = \left(\frac{\omega}{\omega_{\text{ref}}}\right)^{\beta} \tag{14}$$

where ω is the vane rotation rate, with ω_{ref} taken as 0·1 /s.

DISCUSSION

Strain rates relevant for in situ tests, laboratory tests and operational conditions cover an extremely wide range, typically up to six to eight orders of magnitude. For example, suction caissons designed for deep water facilities in the Gulf of Mexico must contend with what are known as 'loop' currents, which may last for several days or even weeks (Clukey *et al.*, 2004). The (nominal) strain rate, v/r_0, associated with shearing along the shaft of a 5 m diameter caisson might thus be $\sim 10^{-8}$ s^{-1} (allowing for 50 mm of movement over a week). This compares with typical strain rates in laboratory testing of 1%/h (or 3×10^{-6} s^{-1}) and nominal strain rates for in situ tests ranging from the vane ($\sim 2 \times 10^{-3}$ s^{-1}) to penetrometers such as the T-bar with velocity changes within the soil of $v/r_0 \sim 1$ s^{-1} (Randolph, 2004).

The analysis presented here is applicable to any shear band (or velocity change) where unlimited broadening of the band would ultimately lead to increased internal plastic work, because of either the greater volume of soil involved, or a less-than-optimum mechanism. An important conclusion is that rate effects are governed not by the absolute velocity change but by the velocity change normalised by the radius of curvature of the shear band. Thus for the vane, contrary to what was assumed by Biscontin & Pestana (2001), it is the rotation rate of the vane rather than the peripheral velocity that controls the rate dependence of the torque.

ACKNOWLEDGEMENTS

This work forms part of the activities of the Centre for Offshore Foundation Systems (COFS), established and supported under the Australian Research Council's Research Centres Program. The first author was supported by an Australian Research Council post-doctoral Fellowship (Discovery Grant DP0558406). The authors would like to acknowledge valuable discussions with Professor Andrew Drescher, who encouraged them to document this work

APPENDIX 1. RIGOROUS ENERGY APPROACH

In the simple energy approach used above, the strain rates within the shear band are assumed constant, given by the average $\dot{\gamma} = \dot{\gamma}(r) = \langle \dot{\gamma} \rangle$. Rigorously, however, the energy approach should leave the function $\dot{\gamma} = \dot{\gamma}(r)$ unknown initially. For example, for the power law rate dependence the general expression for the rate of plastic work ΔP is given by

$$\begin{aligned}\Delta P &= s_{\text{u,ref}} \int_{r_0}^{r_0+t} \dot{\gamma}(r) \left[\frac{\dot{\gamma}(r)}{\dot{\gamma}_{\text{ref}}}\right]^{\beta} r \, \mathrm{d}r \Delta\theta \\ &= \Delta P_0 \int_{r_0}^{r_0+t} L[r, \nu(r), \nu'(r)] \mathrm{d}r\end{aligned} \tag{15}$$

where $\Delta P_0 = s_{\text{u,ref}} \Delta\theta / \dot{\gamma}_{\text{ref}}^{\beta}$ and the integrand

$$L[r, \nu(r), \nu'(r)] = r\left\{-r^{n-1} \frac{\mathrm{d}}{\mathrm{d}r}\left[\nu(r) r^{1-n}\right]\right\}^{\beta+1} \tag{16}$$

Minimisation of the work, this time with respect to the velocity function $v(r)$ rather than the shear band thickness, allows $v(r)$ to be recovered by adopting Euler's formula from variational calculus,

$$\frac{\delta(\Delta P/\Delta P_0)}{\delta \nu(r)} = \frac{\partial L}{\partial \nu(r)} - \frac{\mathrm{d}}{\mathrm{d}r} \frac{\partial L}{\partial \nu'(r)} = 0 \tag{17}$$

which leads to the following differential equation.

$$(\beta - n)(n-1)\nu(r) + (\beta + n - n\beta) r \nu'(r) + \beta r^2 \nu''(r) = 0 \tag{18}$$

Enforcing a boundary condition of zero velocity at large radius, and a velocity of ν_{r_0} at the inner edge, leads to the same result as given by equation (8), such that equilibrium is satisfied.

REFERENCES

Biscontin, G. & Pestana, J. M. (2001). Influence of peripheral velocity on vane shear strength of an artificial clay. *Geotech. Test. J.* **24**, No. 4, 423–429.

Casagrande, A. & Wilson, S. D. (1951). Effect of rate of loading on the strength of clays and shales at constant water content. *Géotechnique* **2**, No. 3, 251–263.

Chandler, R.J. (1988). The in-situ measurement of the undrained shear strength of clays using the field vane. In *Vane shear strength testing of soils: Field and laboratory studies*, ASTM STP 1014, pp. 13–45. West Conshohocken, PA: ASTM International.

Clukey, E. C., Templeton, J. S., Randolph, M. F. & Phillips, R. A. (2004). Suction caisson response under sustained loop-current loads. *Proc. Ann. Offshore Technology Conf., Houston*, Paper OTC 16843.

Graham, J., Crooks, J. H. A. & Bell, A. L. (1983). Time effects on the stress–strain behaviour of natural soft clays. *Géotechnique* **33**, No. 3, 327–340.

Mitchell, J. K. (1993). *Fundamentals of soil behavior*, 2nd edn. New York: Wiley.

Pérez-Foguet, A., Ledezma, A. & Huerta A. (1999). Analysis of the vane test considering size and time effects. *Int. J. Numer. Anal. Methods Geomech.* **32**, No. 5, 383–412.

Prandtl, L. (1921). Eindringungsfestigkeit und festigkeit von schneiden. *Angew. Math. U. Mech.* **1**, No. 15, 15–20.

Randolph, M. F. (2004) Characterisation of soft sediments for offshore applications. *Proc. 2nd Int. Conf. on Site Characterisation, Porto* **1**, 209–231.

Roscoe, K. H. (1970) The influence of strains in soil mechanics. *Géotechnique* **20**, No. 2, 129–170.

Sheahan, T. C., Ladd, C. C. & Germaine, J. T. (1996). Rate-dependent undrained shear behavior of saturated clay. *J. Geotech. Eng. ASCE* **122**, No. 2, 99–108.

Vardoulakis, I. & Graf, B. (1985). Calibration of constitutive models for granular materials using data from biaxial experiments. *Géotechnique* **35**, No. 3, 299–317.